Molecular Dynamics Study on the Reaction of RDX Molecule with Si Substrate

Wei-Sen Xu, Jing Zhu, Yan-Fei Hu, and Guang-Fu Ji*
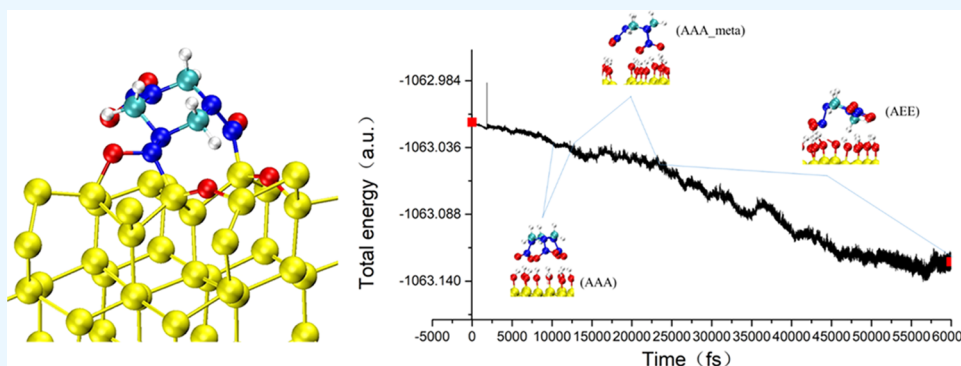
ACCESS | Metrics & More | Article Recommendations

ABSTRACT: RDX is widely used in various explosion situations, and there are many studies on its detonation performance, safety, preparation, etc. Research on preparation of β-RDX is mainly conducted by experiments. In recent years, part of the research points to the use of substrate as a medium to produce β-RDX faster. Based on this guidance, our work aims to theoretically solve the physical and chemical processes that RDX may experience in the production process through numerical simulation. In this work, molecular dynamics simulation is set up for the interaction between RDX and a Si clean surface and a Si hydroxyl saturated surface separately, and a higher precision simulation is set up to verify the reliability of the results. NCI analysis is also used to guess the possible phase transition mechanism in the simulation results. In the simulation process, a 7×7 Si clean surface, a 3×3 Si clean surface, and a 7×7 Si-OH surface are set, and each surface adsorbs one α-RDX. The semiempirical Gfn1-xtb method is used for the 7×7 surface, and the DFT method is used for the 3×3 surface. The calculation results confirmed by high-precision results show that RDX molecules will react with the dangling bonds on the Si surface. Three conformations of RDX were found on the hydroxyl saturated surface of Si. The isosurface generated by the NCI method is used to analyze the reasons for the formation of these conformations.

1. INTRODUCTION

1,3,5-Trinitrohexahydro-s-triazine (RDX, C3H6N6O6) is one of the most commonly used energetic materials because of its good detonation performance and appropriate explosive sensitivity.[1−11] In recent years, many studies have revealed the phase structure of RDX. From a series of experimental and theoretical calculation results, the phase structure of RDX includes the following five types: $\alpha, \beta, \gamma, \delta$, and ε. Here, α-RDX is the stable phase under ambient condition, β-RDX is the metastable phase, which exists near the melting line, and γ, δ, and ε-RDX exist under high pressure.[3,12−21] The conformational differences of RDX molecules in these phases are mainly shown by the different relative positions of nitro groups with respect to the triazine ring. The two most common conformations are AAA (all nitro groups axial to the triazine ring), which forms β-RDX, and AAE (two of the nitro groups axial to the triazine ring, with the third in an equatorial position), which forms α-RDX (Figure 1).
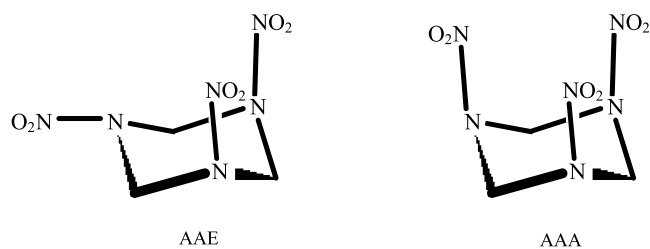

Figure 1. Two conformations of the RDX molecule. The AAA form has all nitro groups axial to the triazine ring, and the AAE form has an equatorial group.
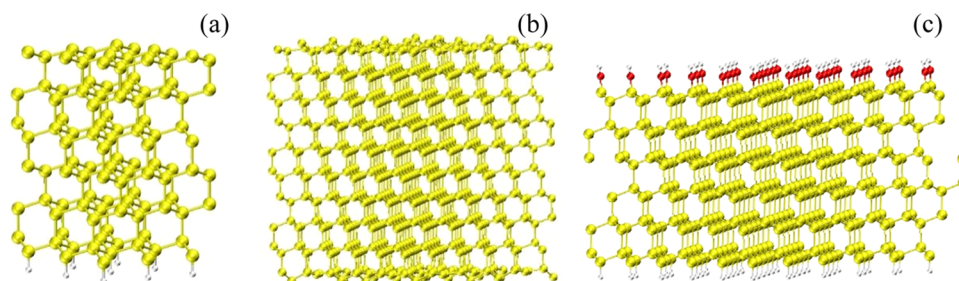
Figure 2. (a) 3×3 silicon surface in the (111) plane. (b) 7×7 silicon surface in the (111) plane saturated by H atoms on the slab's bottom. (c) 7×7 silicon surface in the (111) plane saturated by −OH groups on the slab's upper surface and saturated by H atoms on the bottom.
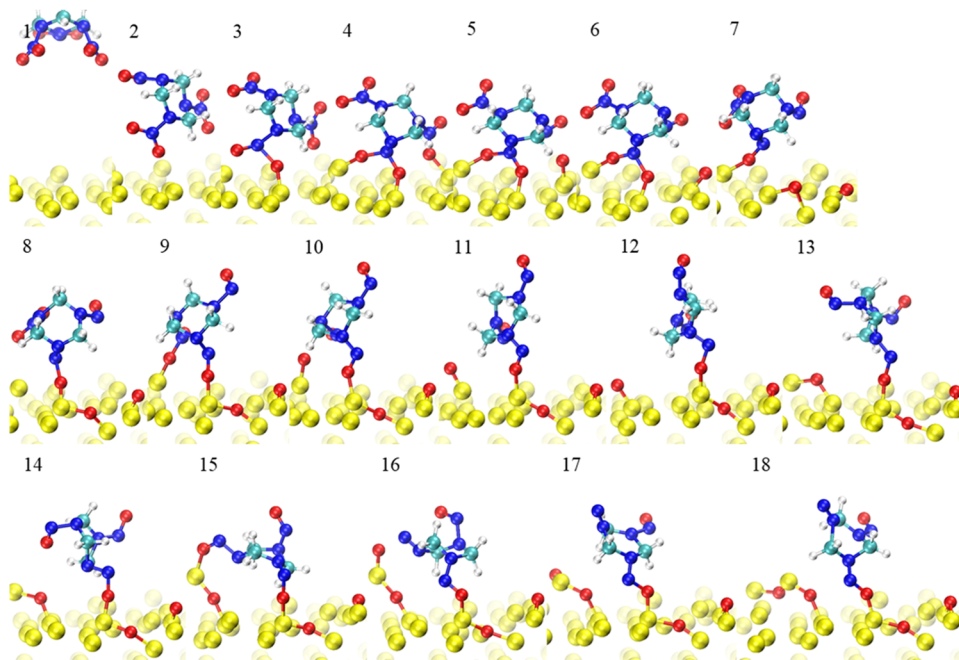

Figure 3. Eighteen frames of the dynamic process of the chemical reaction between the RDX molecule and the 7×7 silicon slab.

In practical use, the $\alpha−\beta$ phase transition of RDX often occurs in various conditions, which are usually related to preparing samples or the safety of EM.[7,9,12,22,23] In some reports, researchers deposited RDX solution onto different substrate surfaces (glass, hydrophilic glass, stainless steel, gold), and the $\alpha−\beta$ phase transition was found in the crystallization process by IR and Raman spectroscopies.[1,17,22,24,25] As a contrast, a density functional theory (DFT) result shows that the RDX molecule on an Al_{16} layer changes the conformation of RDX to nearly AAA, which is indicative of the β form. Gao et al.[26] further studied the growth of the β form on different substrates using the thermal sublimation deposition method. The experiment concluded that hydrophobic materials are prone to producing α-RDX, whereas hydrophilic materials favor the growth of β-RDX.

Although a relatively stable method for the experimental preparation of RDX is already available, we still do not know what physical or chemical processes the RDX molecules undergo on the substrate that may lead to a phase transition.

In this work, first-principles methods and semiempirical quantum chemical methods are used to simulate the kinetic processes and chemical reaction processes of RDX molecules on the three silicon substrates and to analyze the noncovalent interactions (NCIs) in the kinetic process. This work provides a theoretical basis for relevant experimental studies.

2. COMPUTATIONAL DETAILS

To discuss different substrate conditions, we set three kinds of Si surfaces:

(1) Si clean surface, which is modeled as a slab of 20 Si layers, forming a (7×7) surface cell in a (111) plane (Figure 2b).

(2) Si clean surface, which is modeled as a slab of 12 Si layers, forming a (3×3) surface cell in a (111) plane. The Si dangling bonds are saturated by H atoms on the slab's bottom surface (Figure 2a).

(3) Si-OH surface, which is modeled as a slab of 12 Si layers, forming a (7×7) surface cell in a (111) plane. The Si dangling bonds are saturated by −OH groups on the slab's upper surface and saturated by H atoms on the bottom. The last two layers of Si and the H layer at the bottom are fixed (Figure 2c).

Surfaces 1 and 3 are used to simulate the possible effects of different areas of the surface in experiments. Simulation of surface 2 uses a more accurate algorithm to provide a comparison of the chemical reaction process on surface 1. The starting structure adsorbed to the substrate surface is an AAE-type RDX molecule.

All simulations in this work were calculated using the CP2K code.[27] The semiempirical GFN1-xTB[28] method was used to calculate the MD process on surfaces 1 and 3, and the exchange
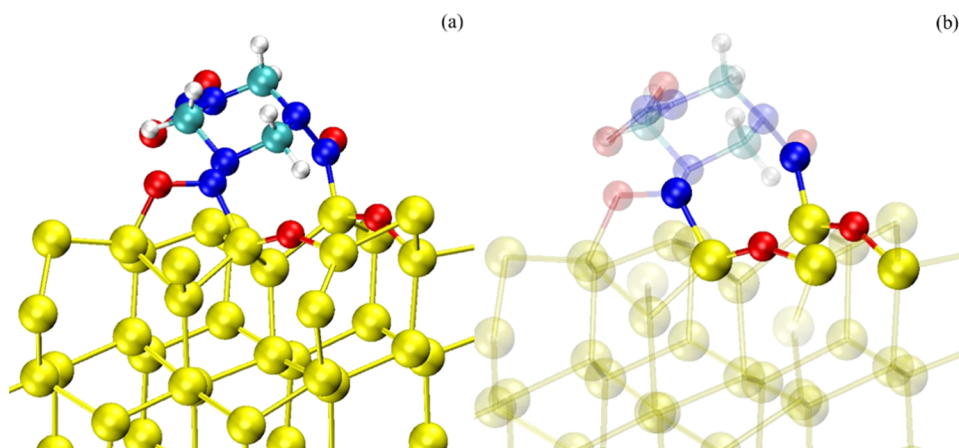
Figure 4. (a) Final state of the reaction between RDX with a 3 × 3 Si substrate. (b) Highlighting of the N−Si bond and the O−Si bond.
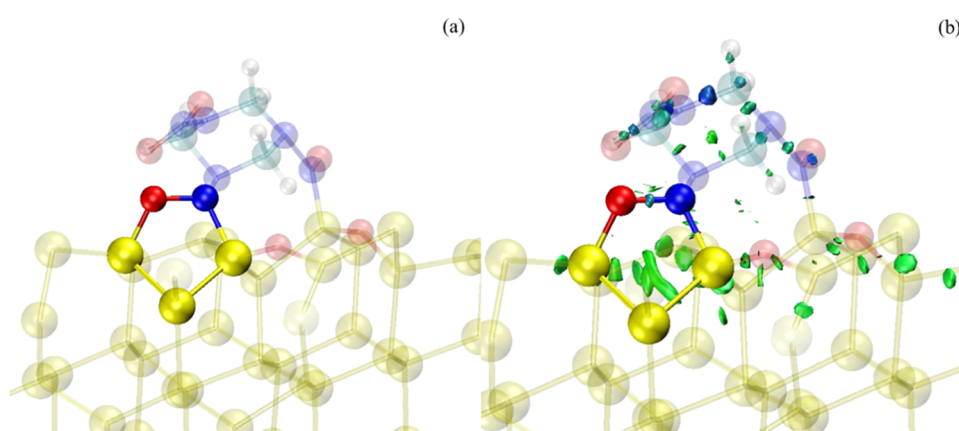

Figure 5. (a) Highlighting the five-element ring in the final state of the reaction between RDX with the 3 × 3 Si substrate. (b) NCI isosurface near and in the center of the five-element ring.

correlation energy was determined using ab initio molecular dynamics (AIMD) combined with the PBE functional.[29] The Goldk−Teter−Hutter (GTH) pseudopotential[30] and the double-ζ-with-polarization (DZVP) base set were used, and the finest grid level cutoff was set to 400 Ry for the Γ point.

Both methods are combined with Grimme's D3 dispersion corrections[31] and the periodic boundary conditions. The time step for all MD motions is set to 1.0 fs, with the NVT ensemble at 300 K. The Nosé−Hoover thermostat is employed for the process on surfaces 1 and 3, and the canonical sampling through velocity rescaling (CSVR) thermostat is set for surface 2. The Multiwfn package is used for wave-function analyses of NCI.[32]

3. RESULTS AND DISCUSSION

3.1. MD Process on Surface 1. Figure 3 shows the dynamic process of the chemical reaction between the RDX molecule and the 7 × 7 Si slab. The whole process is displayed in 18 frames at a total of 3.7 ps. One A-type −NO_2 (nitro groups axial to the triazine ring) and one E-type −NO_2 (nitro groups equatorial to the triazine ring) of the RDX molecule in the AAE configuration first contact the Si surface in frame 3, and the oxygen atom in the A-type −NO_2 starts to bond with the substrate. In the next frame, the O in the E-type −NO_2 goes to the O−Si bond too. Due to the strong reducibility of dangling bonds, the O on the E-type −NO_2 is quickly removed, and the O atom saturates two Si dangling bonds forming a Si−O−Si bond; see frame 6. Then, the O atom in the A-type −NO_2 went through the same process in

frames 7−8. Finally, one O atom of the remaining nitro group is also taken away by Si substrate until frame 11. Now each nitro group on RDX has been taken away by an oxygen atom and turned into −NO, one of which is connected to the Si surface. The −NO without bonding to Si starts to move away from the substrate and drives the whole molecule to flip; see frames 12−13. Perhaps due to the vibration, a Si linked with an O atom flew out of the substrate, bonded with an O on a −NO, and finally reduced the O atom; see frames 14−16. The last two frames show the O−Si−O−Si chain falling back to the substrate and the terminal O atom bonding with another Si.

We can see that at the end of the reaction, the O atoms on the RDX molecule are about to be completely removed, and the Si substrate is partially oxidized. This result shows that the process of preparing β-RDX on the Si substrate may be accompanied by the chemical reaction between RDX and the Si substrate, and finally, the phase transition is caused by the reaction products.

3.2. MD Process on Surface 2. To verify the accuracy of the above process, we used a more accurate first-principles method to perform dynamic calculations and conducted NCI analysis on the calculation results. After AIMD simulation of RDX on the 3 × 3 Si substrate for 2 ps, we found that the initial chemical reaction process of the system is basically consistent with that in Section 3.1. The final state of the system is shown in Figure 4.

Figure 4a shows that one E-type −NO_2 and one A-type −NO_2 both had an O atom removed from the dangling bonds on the surface. Meanwhile, the N atoms in these two nitro groups are

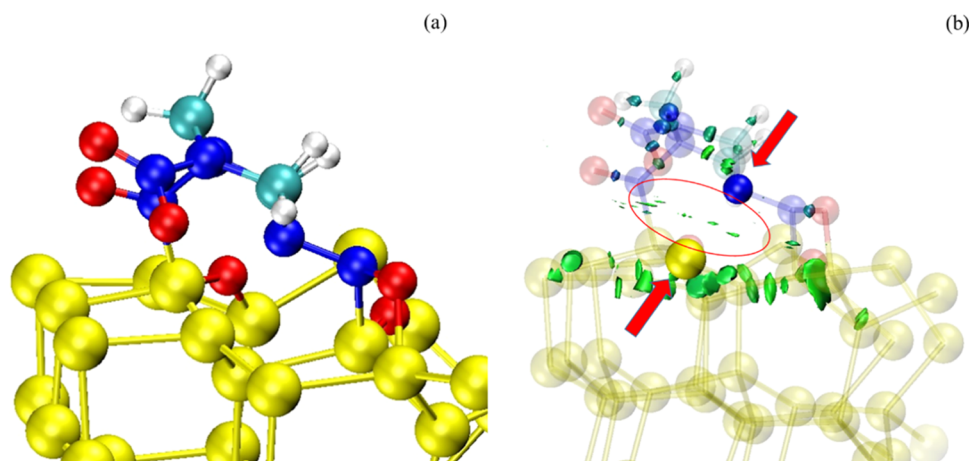(a)   (b)

Figure 6. (a) Lateral view of the final state of the reaction between RDX with the 3 × 3 Si substrate. (b) Sporadic isosurfaces between RDX and the Si surface. The arrow points in the direction of the interaction force.
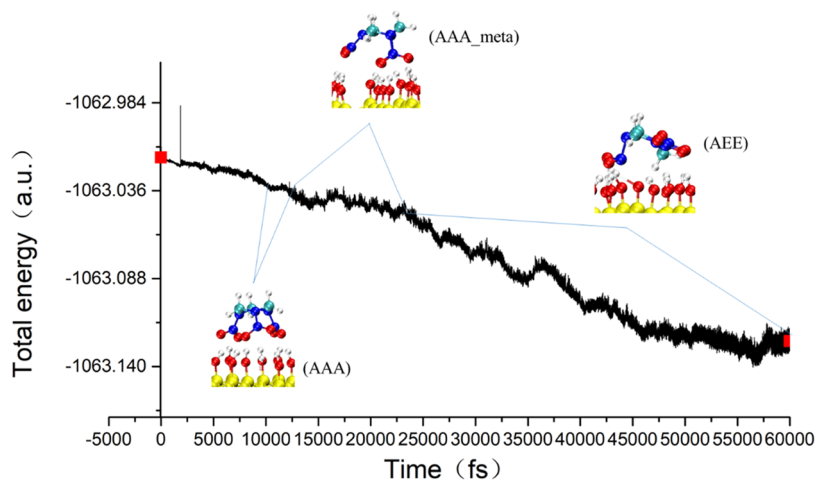

Figure 7. Energy evolution of the RDX dynamic process on the 7 × 7 Si-OH surface with time. Different curve ranges are related to the corresponding RDX conformation.

both bonded to Si atoms below. The oxidation of the silicon surface and the N−Si bond can be clearly seen in Figure 4b.

Since the oxygen atom in the E-type −NO$_2$ also has a bond with Si, the atoms N and O together with Si form a five-membered ring, as seen in Figure 5a.

After the NCI analysis of the reaction area (Figure 5b), it can be seen that there is a small piece of green isosurface in the center of the five-element ring, indicating that the weak interaction will tighten the ring. It means that the N−Si and O−Si bonds will be more stable in this ring.

The chair AAE structure of RDX can be clearly seen from the lateral view (Figure 6a). In this view angle, combined with NCI analysis, it can be seen that there are sporadic isosurfaces between the N atom on the triazine ring and the Si atom below, which implies that there is a certain weak interaction between N and Si along the arrow direction (Figure 6b), so that RDX molecules can cling to the Si surface.

The result of this simulation is almost consistent with the previous results in Figure 3, frames 4−8, which shows that the dynamic process revealed in Section 3.1 is highly reliable. The only difference is that the semiempirical method fails to form a stable N−Si bond, while the N−Si bond under the DFT method seems to be more stable, which may be because the system in Section 3.2 is smaller, and the molecules are not far away from

the surface due to the weak interaction between RDX and its own in the adjacent lattice under periodic conditions.

3.3. MD Process on Surface 3. Considering the possibility that the surface may be affected by moisture or oxidation in reality, it is also necessary to saturate the Si dangling bonds with hydroxyl groups in the simulation. In this simulation, because the system is smaller and there is no chemical reaction, the whole process is relatively stable. A time period of 60 ps was run on the 7 × 7 Si surface saturated with hydroxyl, and three RDX configurations on the surface were obtained except for the initial configuration. Figure 7 shows the evolution of the total energy of the system with time and marks which RDX configuration corresponds to different curve ranges.

First, when the RDX molecule is close to the substrate, its configuration quickly changes from AAE to standard AAA with its energy entering a plateau at the same time. RDX in the AAA configuration is like a bowl covered on the hydroxyl plane (Figure 8a). To further study the cause of AAA formation, a series of isosurfaces have been obtained after NCI analysis near the adsorption point (Figure 8b).

By filtering information, the NCI isosurface is reduced to two types, one is the interaction between oxygen atoms in −NO$_2$ and hydrogen atoms on the hydroxyl surface, and the other is the interaction between nitrogen atoms and oxygen atoms between
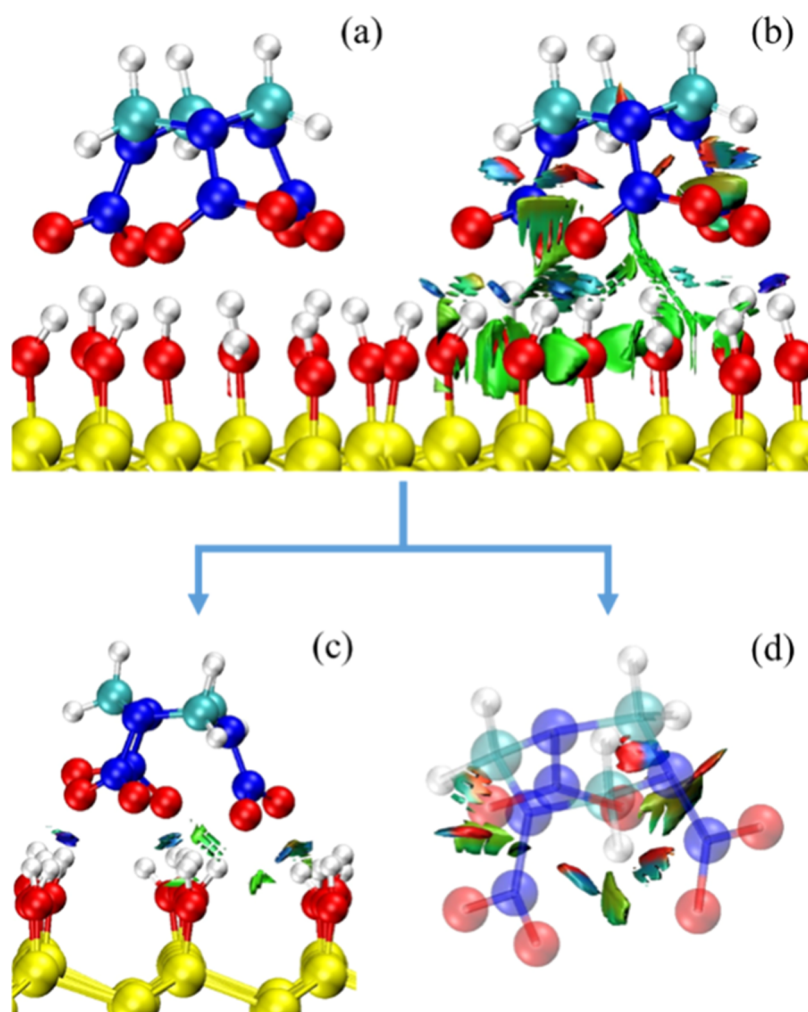
Figure 8. NCI isosurface of AAA conformation of RDX on the 7×7 Si-OH surface and its decomposition. (a) AAA conformation of RDX on the 7×7 Si-OH surface. (b) NCI isosurface of RDX. (c) NCI isosurface of the O atom on RDX and the H atom on the substrate. (d) NCI isosurface of the N atom and the O atom on RDX.
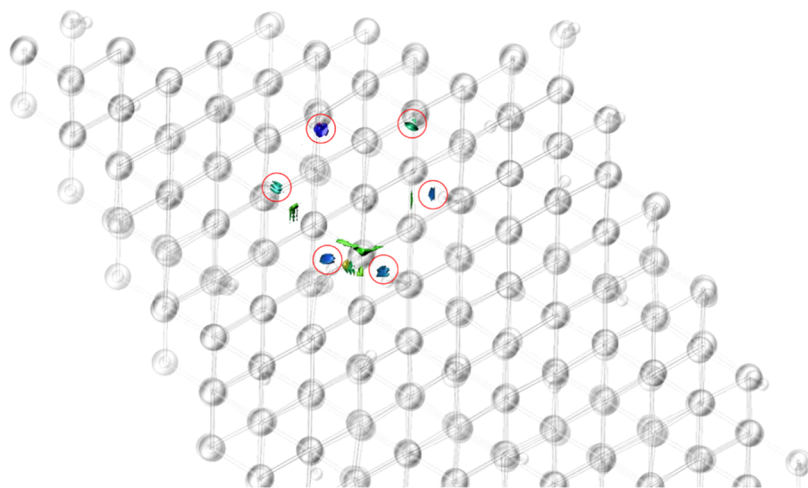

Figure 9. Top view of the NCI isosurface of the O atom on the AAA form RDX and the H atom on the 7×7 Si-OH substrate. The red circle marks the possible hydrogen bonds′ position.

molecules (Figure 8c,d). In Figure 8d, we can see the steric effect represented by the red area of the isosurface, which is also the reason why the AAA conformation can open from the inside like a bowl. Furthermore, after the atoms are virtualized from the top view, we can see the NCI isosurface generated by the contact of six oxygen atoms in three nitro groups with the surface (Figure 9 in the red circle). Most of these isosurfaces are bluish-colored,
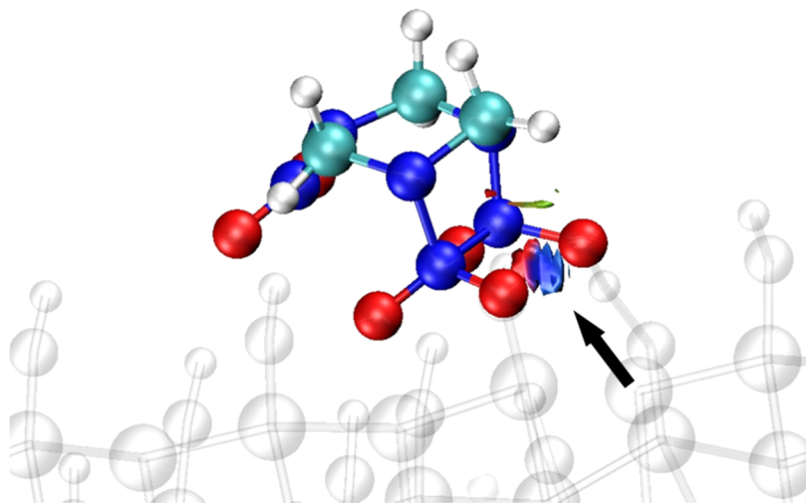
Figure 10. N−N bond and NCI isosurface between two nitro groups of the meta AAA form RDX on the 7 × 7 Si-OH substrate. The arrow points in the position of the isosurface.

indicating a strong interaction that can almost be determined as a hydrogen bond.

After the AAA configuration lasts for a period of time, two nitro groups stick together through each one's N atom, forming an unstable N−N bond, which is because the oxygen atom in −NO$_2$ starts to snatch the hydrogen atom in the hydroxyl surface, leading to a possible charge transfer, finally affecting the electronic architecture. When the N−N bond is formed, the AAA configuration will become a meta type of AAA. The difference between this configuration and AAA is that two nitro groups are absorbed together. Similarly, from the NCI analysis (Figure 10), it can be seen that the isosurface region pointed by the arrow has a steric effect near the N−N bond region and has a probable hydrogen bond near the end of the oxygen atom.

As the oxygen atoms on −NO$_2$ snatch the hydrogen atom more and more frequently on the hydroxyl surface, the two nitro groups that were originally attracted together finally separate after a complex charge rebalancing process. After a long relaxation process, the triazine ring is changed from chair type to boat type. Two nitro compounds originally absorbed together are fully expanded and parallel to the triazine ring. The hybrid orbital of the third nitro group's N atom under the action of the hydrogen bond is from sp^2 to sp^3. The whole molecule presents an AAE conformation. From the NCI image (Figure 11), there are hydrogen bonds between RDX molecules and between molecules and surfaces. The whole molecule is likely fixed on the hydroxyl surface by a hydrogen bond, reaching the lowest and most stable state of energy.

From the energy point of view, after increasing the temperature, the total energy of the system will be closer to the energy platform forming the AAA configuration, and because the hydrogen bond is relatively easier to break, it is more difficult for the system to relax to the lowest energy state of AEE. When the temperature is high enough to easily break the N−N bond under the meta AAA configuration, RDX molecules will maintain the AAA configuration for a long time, which is coincident with the practice in Gao et al.'s article.[26]

4. CONCLUSIONS

We studied the molecular dynamic process of RDX under a Si clean surface, found that RDX molecules will react with the dangling bonds on the Si surface, which will reduce one oxygen
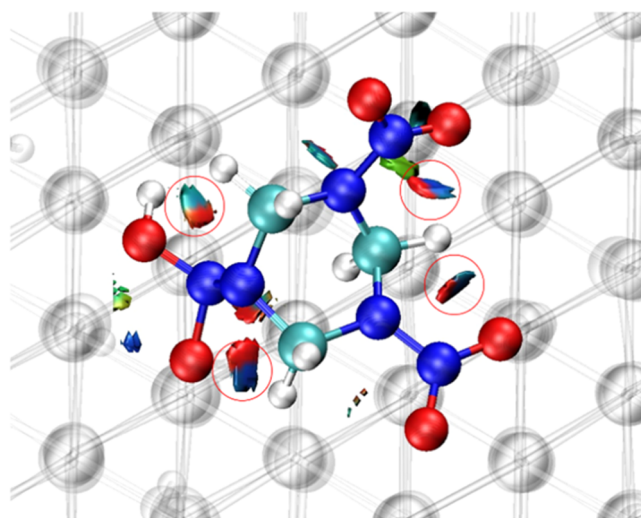

Figure 11. NCI isosurface of AEE form RDX on the 7 × 7 Si-OH substrate. The red circle marks the possible intramolecular hydrogen bonds' position.

atom from each nitro group, and continue to reduce the oxygen atom on NO after one cycle. We then used the first-principles method to obtain more accurate results, and the two results are highly consistent.

On the other hand, we studied the RDX dynamic process on the saturated surface of the Si hydroxyl group and obtained three different RDX conformations, namely, AAA, meta AAA, and AEE. Among them, AAA has the highest energy and AEE has the lowest. According to the results, it can be predicted that under sufficient high-temperature conditions, the conformation may remain in the AAA state for a long time until the crystal nucleus is formed to obtain β-RDX. That is a possible phase transition mechanism, which is interpreted using a first-principles method.

■ AUTHOR INFORMATION

Corresponding Author

Guang-Fu Ji − *Institute of Fluid Physics, China Academy of Engineering Physics, Mianyang 621900, P. R. China*;
Email: cyfjkf@126.com

Authors

Wei-Sen Xu − *Department of Engineering Mechanics, University of Science and Technology of China, Hefei 230026 Anhui, P. R. China; Institute of Fluid Physics, China Academy of Engineering Physics, Mianyang 621900, P. R. China;* orcid.org/0000-0003-4464-6738

Jing Zhu − *Institute of Fluid Physics, China Academy of Engineering Physics, Mianyang 621900, P. R. China*

Yan-Fei Hu − *Department of Applied Physics, Chengdu University of Technology, Chengdu 610059, P. R. China*

Complete contact information is available at:
https://pubs.acs.org/10.1021/acsomega.2c07512

Notes

The authors declare no competing financial interest.

■ REFERENCES

(1) Baer, B. J.; Oxley, J.; Nicol, M. The phase diagram of rdx (hexahydro-1,3,5-trinitro-s-triazine) under hydrostatic pressure. *High Pressure Res.* **1990**, *2*, 99−108.

(2) Miller, P. J.; Block, S.; Piermarini, G. J. Effects of pressure on the thermal decomposition kinetics, chemical reactivity and phase behavior of RDX. *Combust. Flame* **1991**, *83*, 174−184.

(3) Sorescu, D. C.; Rice, B. M.; Thompson, D. L. Intermolecular potential for the hexahydro-1, 3, 5-trinitro-1, 3, 5-s-triazine crystal (RDX): A crystal packing, Monte Carlo, and molecular dynamics study. *J. Phys. Chem. B* **1997**, *101*, 798−808.

(4) Miller, G. R.; Garroway, A. N. *A Review of the Crystal Structures of Common Explosives. Part I: RDX, HMX, TNT, PETN, and Tetryl*, No. NRL/MR/6120-01-8585; Naval Research Lab: Washington DC; 2001.

(5) Vladimiroff, T.; Rice, B. M. Reinvestigation of the gas-phase structure of RDX using density functional theory predictions of electron-scattering intensities. *J. Phys. Chem. A* **2002**, *106*, 10437−10443.

(6) Byrd, E. F.; Rice, B. M. Ab Initio Study of Compressed 1, 3, 5, 7-Tetranitro-1, 3, 5, 7-tetraazacyclooctane (HMX), Cyclotrimethylenetrinitramine (RDX), 2, 4, 6, 8, 10, 12-Hexanitrohexaazaisowurzitane (CL-20), 2, 4, 6-Trinitro-1, 3, 5-benzenetriamine (TATB), and Pentaerythritol Tetranitrate (PETN). *J. Phys. Chem. C* **2007**, *111*, 2787−2796.

(7) Patterson, J. E.; Dreger, Z. A.; Gupta, Y. M. Shock wave-induced phase transition in RDX single crystals. *J. Phys. Chem. B* **2007**, *111*, 10897−10904.

(8) Bedrov, D.; Hooper, J. B.; Smith, G. D.; Sewell, T. D. Shock-induced transformations in crystalline RDX: A uniaxial constant-stress Hugoniostat molecular dynamics simulation study. *J. Chem. Phys.* **2009**, *131*, No. 034712.

(9) An, C.-W.; Li, F.-S.; Song, X.-L.; Wang, Y.; Guo, X.-D. Surface Coating of RDX with a Composite of TNT and an Energetic-Polymer and its Safety Investigation. *Propellants, Explos., Pyrotech.* **2009**, *34*, 400−405.

(10) Wei, H.; He, C.; Zhang, J.; Shreeve, J. M. Combination of 1,2,4-Oxadiazole and 1,2,5-Oxadiazole Moieties for the Generation of High-Performance Energetic Materials. *Angew. Chem. Int. Ed.* **2015**, *54*, 9367−9371.

(11) Ghosh, M.; Banerjee, S.; Shafeeuulla Khan, M. A.; Sikder, N.; Sikder, A. K. Understanding metastable phase transformation during crystallization of RDX, HMX and CL-20: experimental and DFT studies. *Phys. Chem. Chem. Phys.* **2016**, *18*, 23554−23571.

(12) Castillo, R. I. *Theoretical and Experimental Vibrational and NMR Studies of α and β-RDX. dissertation*; University of Puerto Rico, 2008.

(13) Davidson, A. J.; Oswald, I. D. H.; Francis, D. J.; Lennie, A. R.; Marshall, W. G.; Millar, D. I. A.; Pulham, C. R.; Warren, J. E.; Cumming, A. S. Explosives under pressure—the crystal structure of γ-RDX as determined by high-pressure X-ray and neutron diffraction. *CrystEngComm* **2008**, *10*, 162−165.

(14) Miao, M. S.; Dreger, Z. A.; Winey, J. M.; Gupta, Y. M. Density functional theory calculations of pressure effects on the vibrational structure of alpha-RDX. *J. Phys. Chem. A* **2008**, *112*, 12228−12234.

(15) Millar, D. I.; Oswald, I. D.; Francis, D. J.; Marshall, W. G.; Pulham, C. R.; Cumming, A. S. The crystal structure of beta-RDX-an elusive form of an explosive revealed. *Chem. Commun.* **2009**, *5*, 562−564.

(16) Millar, D. I.; Oswald, I. D.; Barry, C.; Francis, D. J.; Marshall, W. G.; Pulham, C. R.; Cumming, A. S. Pressure-cooking of explosives–the crystal structure of epsilon-RDX as determined by X-ray and neutron diffraction. *Chem. Commun.* **2010**, *46*, 5662−5664.

(17) Goldberg, I. G.; Swift, J. A. New Insights into the Metastable *β* Form of RDX. *Cryst. Growth Des.* **2012**, *12*, 1040−1045.

(18) Pereverzev, A.; Sewell, T. D.; Thompson, D. L. Molecular dynamics study of the pressure-dependent terahertz infrared absorption spectrum of alpha- and gamma-RDX. *J. Chem. Phys.* **2013**, *139*, No. 044108.

(19) Wu, Q.; Zhu, W.; Xiao, H. Periodic DFT study of structural, electronic, absorption, and thermodynamic properties of crystalline *α*-RDX under hydrostatic compression. *Struct. Chem.* **2013**, *25*, 451−461.

(20) Sorescu, D. C.; Rice, B. M. RDX Compression, *α→ γ* Phase Transition, and Shock Hugoniot Calculations from Density-Functional-Theory-Based Molecular Dynamics Simulations. *J. Phys. Chem. C* **2016**, *120*, 19547−19557.

(21) Gao, C.; Zhang, C.; Sui, Z.et al. Phase Transition of RDX Under High Pressure Upto 50 GPa. In *26th ICDERS* Boston, MA, USA, 2017.

(22) Torres, P.; Mercado, L.; Cotte, I.; Hernández, S. P.; Mina, N.; Santana, A.; †, R. T. C.; Richard Lareau, A.; Castro, M. E. Vibrational Spectroscopy Study of *β* and *α* RDX Deposits. *J. Instrum. Anal.* **2004**, *25*, 935−936.

(23) Infante Castillo, R.; Pacheco Londoño, L. C.; Hernández Rivera, S. P. Monitoring the *α→β* solid−solid phase transition of RDX with Raman spectroscopy: A theoretical and experimental study. *J. Mol. Struct.* **2010**, *970*, 51−58.

(24) Figueroa-Navedo, A. M.; Ruiz-Caballero, J. L.; Pacheco-Londoño, L. C.; Hernández-Rivera, S. P. Characterization of *α*- and *β*-RDX Polymorphs in Crystalline Deposits on Stainless Steel Substrates. *Cryst. Growth Des.* **2016**, *16*, 3631−3638.

(25) Ruiz-Caballero, J. L.; Aparicio-Bolano, J. A.; Figueroa-Navedo, A. M.; Pacheco-Londono, L. C.; Hernandez-Rivera, S. P. Optical Properties of beta-RDX Thin Films Deposited on Gold and Stainless Steel Substrates Calculated from Reflection-Absorption Infrared Spectra. *Appl. Spectrosc.* **2017**, *71*, 1990−2000.

(26) Gao, C.; Yang, L.; Zeng, Y.; Wang, X.; Zhang, C.; Dai, R.; Wang, Z.; Zheng, X.; Zhang, Z. Growth and Characterization of *β*-RDX Single-Crystal Particles. *J. Phys. Chem. C* **2017**, *121*, 17586−17594.

(27) VandeVondele, J.; Krack, M.; Mohamed, F.; Parrinello, M.; Chassaing, T.; Hutter, J. Quickstep: Fast and accurate density functional calculations using a mixed Gaussian and plane waves approach. *Comput. Phys. Commun.* **2005**, *167*, 103−128.

(28) Grimme, S.; Bannwarth, C.; Shushkov, P. A Robust and Accurate Tight-Binding Quantum Chemical Method for Structures, Vibrational Frequencies, and Noncovalent Interactions of Large Molecular Systems Parametrized for All spd-Block Elements (Z = 1-86). *J. Chem. Theory Comput.* **2017**, *13*, 1989−2009.

(29) Perdew, J. P.; Burke, K.; Ernzerhof, M. Generalized gradient approximation made simple. *Phys. Rev. Lett.* **1996**, *77*, 3865.

(30) Goedecker, S.; Teter, M.; Hutter, J. Separable dual-space Gaussian pseudopotentials. *Phys. Rev. B: Condens. Matter Mater. Phys.* **1996**, *54*, No. 1703.

(31) Grimme, S.; Antony, J.; Ehrlich, S.; Krieg, H. A consistent and accurate ab initio parametrization of density functional dispersion correction (DFT-D) for the 94 elements H-Pu. *J. Chem. Phys. A* **2010**, *132*, No. 154104.

(32) Lu, T.; Chen, F. Multiwfn: a multifunctional wavefunction analyzer. *J. Comput. Chem.* **2012**, *33*, 580−592.